JPET Fast Forward. Published on June 10, 2004 as DOI: 10.1124/jpet.104.070011

Disposition Kinetics of Propranolol Isomers in the Perfused Rat Liver

Daniel Y. Hung, Gerhard A. Siebert, Ping Chang, Yuri G. Anissimov and Michael S. Roberts

Department of Medicine, Princess Alexandra Hospital, University of Queensland, Woolloongabba, Queensland, Australia.

JPET Fast Forward. Published on June 10, 2004 as DOI: 10.1124/jpet.104.070011
This article has not been copyedited and formatted. The final version may differ from this version.

Running title: Hepatic propranolol isomers disposition kinetics

Author for correspondence: Professor Michael S. Roberts

Department of Medicine, University of Queensland, Princess Alexandra Hospital, Woollongabba, Qld 4102, Australia.

Telephone: 61-7-32402546; Facsimile: 61-7-32405399

Email: M.Roberts@mailbox.uq.edu.au

Number of text pages: 27

Number of tables: 5

Number of figures: 7

Number of references: 27

Number of words in Abstract: 185

Number of words in Introduction: 299

Number of words in Discussion: 1689

List of Abbreviations

CL_{int}	intrinsic elimination clearance	PS	permeability-surface area product
K_b	equilibrium amount ratio characterising the intracellular binding sites	V_B	extracellular reference space
K_v	equilibrium amount ratio characterising the vesicular ion-trapping sites (ion-trapping parameter)	V_C	cellular water volume

Abstract

The aim of this study was to define the determinants of the linear hepatic disposition kinetics of propranolol optical isomers using a perfused rat liver. Monensin was used to abolish the lysosomal proton gradient to allow an estimation of propranolol ion-trapping by hepatic acidic vesicles. *In vitro* studies were used for independent estimates of microsomal binding and intrinsic clearance. Hepatic extraction and mean transit time were determined from outflow-concentration profiles using a non-parametric method. Kinetic parameters were derived from a physiologically based pharmacokinetic model. Modelling showed an approximate 34-fold decrease in ion-trapping following monensin treatment. The observed model-derived ion-trapping was similar to estimated theoretical values. No differences in ion-trapping values was found between R(+) and S(-) propranolol. Hepatic propranolol extraction was sensitive to changes in liver perfusate flow, permeability-surface area product and intrinsic clearance. Ion-trapping, microsomal and non-specific binding and distribution of unbound propranolol accounted for 47.4%, 47.1% and 5.5% of the sequestration of propranolol in the liver, respectively. It is concluded that the physiologically more active S(-)-propranolol differs from the R(+) isomer in higher permeability-surface area product, intrinsic clearance, and intracellular binding site values.

Introduction

Propranolol is a widely used nonselective beta-blocking agent which is highly extracted in the liver (Shand, 1976) and exhibits a non-linear first pass metabolism in the rat (Suzuki et al., 1981) due to saturation of hepatic tissue binding (Anderson et al., 1978; Miyauchi et al., 1993) and Michaelis-Menten metabolic enzyme or sequestration clearance (Keiding and Steiness, 1984; Smallwood et al., 1988) as well as metabolic stereo-selectivity. It has been described as a 'problematic' drug in terms of its first-pass metabolism not being properly described (Lalka et al., 1993).

As the stereo-selective elimination of propranolol enantiomers remains poorly understood (Marier et al., 1998) and as propranolol is marketed as a racemate consisting of the two enantiomers, we examined the contribution of the stereochemistry of propranolol on its hepatic disposition kinetics by investigating the individual disposition kinetics of both R(+) and S(-)-propranolol and the racemate after bolus injection in the single-pass perfused rat liver. In addition, we measured the microsomal protein binding and metabolism of individual propranolol isomers in an *in vitro* study. These *in vitro* data were then used to validate the hepatic disposition kinetic model derived from the *in situ* impulse-response studies using perfusate concentrations.

This study follows our recently reported structure-hepatic disposition relationships of several cationic drugs in the normal and the diseased rat liver (Hung et al., 2001; Hung et al., 2002) and here we also determined pharmacokinetic parameters such as hepatocellular influx, efflux, binding and elimination for these optical isomers. Kinetic parameters were derived from a two-phase physiologically based organ pharmacokinetic model (Weiss and Roberts, 1996; Hung et

al., 2001). Of particular interest was fully defining the determinants of propranolol isomer hepatic extraction and mean transit time at non-saturable propranolol concentrations, including the relative contribution of ion-trapping and microsomal binding to the uptake of propranolol isomers.

Material and Methods

Chemicals

Monensin sodium (2-[5-ethyltetrahydro-5-[tetrahydro-3-methyl-5-[tetrahydro-6-hydroxy-6-(hydroxymethyl)-3,5-dimethyl-2H-pyran-2-yl]-2-furyl]-2-furyl]-9-hydroxy-β-methoxy-α,γ,2,8-tetramethyl-1,6-dioxaspiro[4,5]decane-7-butyric sodium salt), S(-)-propranolol (1-[(1-methylethyl)amino]-3-(1-naphtalenyloxy)-2-propanol), R(+)-propranolol, and RS-propranolol all were obtained from Sigma Chemical Co., St Louis, MO. [U-^{14}C]DMO (dimethyloxazolidine-2,4-dione), [U-^{14}C]sucrose, [^{3}H]water were purchased from Amersham, Buckinghamshire, UK.

In situ perfusion of the isolated rat liver

Perfusion of the isolated rat liver used in this study was performed as described elsewhere (Cheung et al., 1996). Briefly, male Wistar rats, weighing 200-250 g were anaesthetised using an intraperitoneal injection of xylazine/ketamine (10/80 mg kg^{-1}). The laparatomised rats were heparinized with 200 units heparin injected into the inferior vena cava. The bile duct and the portal vein were cannulated (PE-10, Clay Adams, Franklin Lakes, NJ) and using an intravenous 16-gauge catheter, respectively. The liver was then perfused with MOPS [3-(N-morpholino-)propanesulfonic acid]-buffer containing 2% BSA and 15% washed canine red blood cells (RBC), adjusted to pH 7.40 and oxygenated via a silastic tubing lung, ventilated with an atmosphere of 100% pure oxygen. A peristaltic pump was used as non-circulating perfusion system. The animals were sacrificed by thoracotomy once perfusion was established and the inferior vena cava was cannulated for collection of samples. The animals were placed in a temperature-controlled environment at 37^{o}C. Assessment of liver viability was by macroscopic appearance, measurement of bile flow, oxygen consumption and portal resistance pressure (Cheung et al., 1996).

Perfusions were adjusted to a flow rate of 15 ml/min and given a 10-min period to stabilise before the injection of the first bolus. Aliquots (50 μL) of perfusion medium containing a particular propranolol optical isomer (0.06-0.11 μmole as determined by HPLC assay), [U-^{14}C]sucrose ($1.5x10^6$ dpm) or [U-^{14}C]DMO ($1.5x10^6$ dpm), and [^{3}H]water ($3x10^6$ dpm) was injected into the liver with outlet samples collected via a fraction collector over 4 min (1 sec x 20, 4 sec x 5, 10 sec x 5, 30 sec x 5). The injection was timed to coincide with the start of a computer-controlled fraction collector (samples were collected over 4 min: 20 x 1 s, 5 x 4 s, 5 x 10 s, 4 x 30 s). Up to 6 bolus injections in randomised order were administered per liver. The total perfusion time was less than two hours. Rats in the treatment group received a 10 min perfusion of 0.5 mM (final concentration) monensin/methanol in buffer/RBC and controls were perfused for 10 min with buffer/RBC.

The collected samples were centrifuged and 75 μL aliquots of the supernatant containing [^{3}H]water, [U-^{14}C]sucrose, or [^{14}C]DMO were taken for scintillation counting (MINAXI beta TRI-CARB 4000 series liquid scintillation counter, Packard Instruments Co., USA). The remainder was vortexed and treated with TCA (trichloroacetic acid) /mobile phase (1:2) for HPLC analysis to determine the R(+)-propranolol, S(-)-propranolol or RS-propranolol outflow concentrations.

Perfusion medium binding

Experiments to determine propranolol optical isomer binding were carried out using 2% BSA MOPS buffer (pH 7.4) containing 15% (v/v) pre-washed canine red blood cells. The unbound fraction of the three propranolol optical isomers was determined using an ultra-filtration of a 1

µM perfusate solution. 500 µl aliquots (in triplicate) were placed in a Microcon centrifugal filter device with a nominal molecular weight limit of 10,000 Daltons (Amicon, Beverly, Ma) and centrifuged at 3000 x g for 30 minutes. The content of the filtrate was assayed by HPLC. The unbound fraction of optical isomer was determined as the ratio of free drug to the total concentration.

In vitro binding and metabolism of microsomal protein

To assess the effect of monensin on hepatic drug binding and metabolism an *in vitro* study with a microsomal protein preparation in the presence and absence of monensin was carried out, using buffer containing 0.35 mg/ml microsomal protein from normal livers. The unbound fraction of individual propranolol optical isomer in each buffer solution was estimated using an ultra-filtration method. A known concentration of the individual propranolol optical isomer stock solution was added to 500 µl of each buffer solution to make final concentration of 0.05 µM and placed in a centrifugal filter device (Microcon YM-30, 30,000 MWCO, Millipore Corp., Bedford, MA) and then centrifuged at 3000 x g for 10 min. The ultra-filtrate (in triplicate) was assayed by HPLC. The unbound fraction (f_{uB}) was determined as the ratio of the free concentration to total concentration of solute.

The impact of monensin on hepatic drug metabolism was assessed by incubation of 0.06-0.11 µmole of each propranolol isomer with microsomal protein (0.35 mg/ml) at 37^{o}C. Samples were then collected at 0, 5, 10 and 20 min. The concentration in supernatant after centrifugation determined by HPLC and the logarithm of the concentration remaining in solution plotted against time to obtain a slope and an extrapolated initial concentration (at time zero). Linearity of the relationship and an extrapolated initial concentration being much less than the reported

Michaelis-Menten constant for propranolol (Ishida et al., 1992) was used to confirm linear kinetics. The intrinsic elimination clearance (CL_{int}) was estimated as the product of the slope and the dose divided by the extrapolated initial concentration.

Analytical procedure

The high performance liquid chromatography (HPLC) method employed in this work has been described and validated previously (Hung et al., 2001).

Data analysis

A two-phase physiologically based organ pharmacokinetic model was used to analyse propranolol isomer disposition in the perfused liver. This model, which describes inter-sinusoidal mixing also called vascular dispersion (Roberts et al., 1988), transfer across a permeability barrier, and the intracellular distribution and elimination kinetics (Weiss and Roberts, 1996; Weiss et al., 1997), has been previously applied to the disposition of diclofenac (Weiss et al., 2000). In present work this model (as shown in Fig. 1 and Equation 1) has been developed to accommodate both ion-trapping (K_v, characterizing the vesicular ion-trapping sites) and intracellular binding (K_b, characterizing the intracellular binding sites) for model cationic drugs. The underlying mathematics of the model and the estimation of relative contribution of ion-trapping, microsomal binding and distribution of unbound drug for hepatic sequestration of propranolol have been described in detail previously (Siebert et al., 2004).

$$\hat{f}_y(s) = \frac{(s + k_{vc})k_{in}}{s^2(k_{in}/k_{out})(1+K_b) + s((k_{in}/k_{out})(k_{vc} + K_b k_{vc} + k_e + k_{cv}) + k_{in}) + (k_{in}/k_{out})k_e k_{vc} + k_{in}k_{vc}} \quad (1)$$

where the permeation rate constant, $k_{in} = f_{uB}PS/V_B$, is the permeation clearance per extracellular volume V_B, PS is the permeability-surface area product. k_{out} is the efflux rate constant. The equilibrium amount ratio $K_v = k_{cv}/k_{vc}$ characterises the slowly accessible pool for ion-trapping, K_b is defined as a rapidly equilibrating intracellular binding sites (microsomal and non-specific binding). k_{cv} and k_{vc} represent the rate constant for transport from cytosol into acidic vesicles (lysosomes and mitochondria) or from acidic vesicles into cytosol, respectively. The elimination rate constant defined as $k_e = CL_{int}/V_C$ is the intrinsic elimination clearance normalised per cellular volume V_C (Hung et al., 2001). Data were fitted and calculated using Scientist (Micromath Scientist, Salt Lake City, UT).

Intracellular pH (pH_i) was calculated from the concentration outflow profiles for [^{14}C]DMO, [U-^{14}C]sucrose and [^{3}H]water using an adaptation of the method of Le Couteur et al (Le Couteur et al., 1993). Briefly, the relationship

$$pH_i = \log\left[p\left(10^{pHe} + 10^{6.13}\right) - 10^{6.13}\right] \quad (2)$$

where p is the distribution ratio of DMO described as

$$p = \frac{MTT_{DMO} - MTT_{sucrose}}{MTT_{water} - MTT_{sucrose}} \quad (3)$$

6.13 is the pK_a of DMO and 7.4 is the pK_a of pH_e (extracellular pH) used for the estimation of pH_i.

Sensitivity analyses

The predicted extraction ratio and mean transit time defined by two-phase physiologically based pharmacokinetic model (E_{pred} and MTT_{pred}) are defined by Equations (4) and (5):

JPET Fast Forward. Published on June 10, 2004 as DOI: 10.1124/jpet.104.070011
This article has not been copyedited and formatted. The final version may differ from this version.

$$E_{pred} = 1 - pG_1 - (1-p)G_2 \quad (4)$$

where p is the fraction of the Laplace transform of a sum of 2 inverse Gaussian density functions (G_1 and G_2) for vascular references not entering hepatocytes.

$$MTT_{pred} = \frac{g_p}{pG_1 + (1-p)G_2}\left[\frac{G_1 pMTT_1}{\sqrt{1+2CV^2{}_1 MTT_1 R_N}} + \frac{G_2(1-p)MTT_2}{\sqrt{1+2CV^2{}_2 MTT_2 R_N}}\right] \quad (5)$$

where CV^2 is the normalized variance, R_N is the efficiency number which characterizes the elimination of solute by the liver,

$$g_p = 1 + \frac{k_{in}k_{out}\left(1+K_b+k_{cv}/k_{vc}\right)}{\left(k_{out}+k_e\right)^2},\ R_N = \frac{k_e k_{in}}{k_e + k_{out}}, \quad (6)$$

$$G_i = \exp\left\{\frac{1}{CV_i^2} - \left[\frac{MTT_i}{CV_i^2/2}\left(R_N + \frac{1}{2MTT_i CV_i^2}\right)\right]^{1/2}\right\} \ (i=1,2) \quad (7)$$

In the sensitivity analysis, the effects of altering the parameters defining hepatic disposition on *E* and *MTT* of propranolol was examined for RS-propranolol by changing the individual model parameter values derived to define propranolol disposition in the perfused liver.

Statistical analysis

All data are presented as mean ± standard deviation. Statistical analysis was performed using a two-way analysis of variance to assess the presence of significance between the control and treatment groups followed by Tukey's post hoc test (including the Kramer extension) to identify the source of the significance within the group. Statistical significance was taken at the level $p<0.05$.

Results

Fig. 2A shows a typical R(+)-propranolol and [U-^{14}C]sucrose outflow perfusion concentration-time profile in the regressions (data weighted, $1/y_{obs}^2$). [U-^{14}C]sucrose was co-administered as an extracellular reference solute in the same bolus injection The fit was obtained by the equations described in the section of data analysis. It is evident that the model gives a good fit for the data. The perfusate data appear to have at least three phases (rapid up phase, fast down phase and slow down phase). The corresponding S(-)-propranolol and [U-^{14}C]sucrose perfusate concentration-time data and model regressions are shown in Fig. 2B. The profiles are similar to the R(+) profile but with the perfusate outflow fractions being slightly lower.

Fig. 3 shows a comparison of typical measured and predicted (fitted data) outflow perfusion concentration-time profiles before and after monensin treatment for the propranolol R(+) and S(-) enantiomers and racemic propranolol using co-administered [U-^{14}C]sucrose and [^{3}H]water for estimation of extracellular and cellular volumes. It is apparent that monensin pre-treatment greatly broadened the peak of the outflow profiles compared to controls. Data points measured and data regression lines predicted by the two-phase organ model appeared adequately fitted (Fig. 3A-C). Also shown in Fig. 3 that data points and predicted regression lines for both enantiomers and racemic propranolol increased following monensin administration.

Table 1 shows the non-parametric moments parameters for the drugs used in the study. No significant differences between control and monensin-treated groups were observed for hepatic extraction ratio and normalized variance for the propranolol optical isomers. However, there was a significant difference in mean transit time between control and treatment groups (Table

1). No significant differences for the non-parametric parameters were found to exist between the two propranolol enantiomers and racemic propranolol (Table 1).

Table 2 summarizes the kinetic parameters derived from the two-phase organ model for hepatic drug disposition of propranolol enantiomers and racemic propranolol. The vesicular ion-trapping constant K_v significantly decreased following monensin treatment for R(+)-propranolol, S(-)-propranolol and racemic propranolol (K_v control/K_v treatment: 33-, 34- and 35-fold, respectively). However, no changes following monensin treatment were observed for intrinsic elimination clearance (CL_{int}), permeability-surface area product (PS), or intracellular binding constant (K_b) values for all optical isomers.

Table 2 also compares the stereo-selectivity of the R(+) and S(-) enantiomer and the propranolol racemate. It shows that the S(-)-isomer has significantly higher PS, $CL_{int,}$ and K_b values than those of R(+)-isomer but a comparable K_v value to R(+)-isomer. The kinetic parameters PS, CL_{int}, and K_b values were found to be increased 1.5-, 1.4-, and 1.2-fold, respectively, for the S(-)-propranolol compared to the R(+) enantiomer, reflecting a more pronounced disposition of the S(-) enantiomer in liver tissue. However, no significant difference was found to exist between S(-)-propranolol and RS-propranolol.

Table 3 shows the results of the *in vitro* drug binding and drug metabolism study. Monensin did not affect binding or metabolic activity *in vitro* for all three optical isomers. The calculated CL_{int} and fraction of drug unbound values for the R(+)-propranolol were statistically different ($p<0.05$) to those of S(-)-propranolol and RS-propranolol both in the control and treatment groups.

The determination of the intracellular pH showed no statistically significant differences before and after monensin treatment (7.34 ± 0.19 and 7.27 ± 0.06, respectively).

Table 4 shows the predicted and observed model-derived ion-trapping parameter K_v values. The observed values were found to be very similar to the theoretical values. No differences in K_v values were found between R(+) and S(-) propranolol.

A sensitivity analysis on the effects of changing the individual model parameter values for RS-propranolol suggests that hepatic extraction is significantly affected by metabolism (k_e, $p<0.05$), permeability ($p<0.05$) and blood flow ($p<0.05$) but not intracellular binding (K_b) and ion-trapping (K_v, Table 5). In contrast, the mean transit time is significantly affected by K_v ($p<0.01$) and K_b ($p<0.05$, Table 5). Both the simulated control and monensin-treated groups had similar predicted hepatic extraction and mean transit time values as those obtained from the non-parametric moments analysis (Table 5). An analysis of the outflow perfusion concentration-time profiles in the control and the monensin-treated groups (Fig. 3C) yielded a significant difference in K_v (Table 2) and such a difference also leads to a model predicted differences in mean transit time which are consistent with moment estimations (Table 5).

Discussion

In this study a physiologically based two-phase organ pharmacokinetic model was used to account for vascular dispersion, hepatic permeability, ion-trapping by subcellular acidic organelles, intracellular binding and intrinsic metabolic clearance of propranolol in the perfused rat liver (Roberts et al., 1988). Resolution of the relative concentration of each transport process by the model followed the conduct of impulse-response profiles of propranolol in control and monensin-treated livers, the propranolol being administered at a sufficiently low dose to avoid a non-linearity in plasma protein binding (Ludden, 1991), liver binding (Anderson et al., 1978; Miyauchi et al., 1993) or in hepatic metabolism, recognizing that a range of Michaelis constants need to be incorporated under saturable conditions (Ishida et al., 1992). The model gave a good fit of the data with and without monensin treatment (Fig. 3) and yielded predicted values of hepatic extraction and mean transit time, consistent with model independent moment estimates (Table 5). The individual propranolol enantiomer perfusate concentration-time profile is similar in shape to that observed for the racemate that we have reported earlier (Siebert et al., 2004). It is evident that monensin increases the peak propranolol outflow concentration and abolishes the initial subsequent rapid decline in outflow concentrations after dosing (Fig. 3). As is evident from the binding and transport kinetic data derived in Tables 2 and 3, monensin's effect can be attributed almost exclusively to its reducing the distribution of propranolol into acidic cell organelles.

A further clarification on the disposition of propranolol isomers in the liver is possible from analysis of outflow profiles and the amount of propranolol isomer remaining in the liver over time. Under hypoxic conditions, the metabolism of propranolol is considerably compromised (Elliott et al., 1993) so that it becomes possible to sacrifice liver perfusions at various times and measure propranolol isomer concentrations in the liver at those times. The overall outflow

profiles obtained in our laboratory using red blood cell free perfusate yielded a similar shape profiles as found for control livers but with a much slower terminal phase. Hypoxia therefore did not appear to affect either the peak outflow concentration or subsequent rapid decline and therefore contrasts with the data obtained with monensin in this work. Analysis of the tissue concentrations showed that the S-isomer has higher tissue levels than the R-isomer, consistent with the high binding to liver proteins as suggested by the *in vitro* studies (Table 3) and previously reported data (Anderson et al., 1978). An analysis of propranolol tissue levels over time revealed that the logarithm of the propranolol tissue concentrations decline in a linear manner over time further confirming that the propranolol concentrations used in this work were below those causing saturation.

Stereo-selectivity in the disposition of propranolol enantiomers in the perfused liver is evident for *PS*, CL_{int} and K_b but not K_v. Ion-trapping accounts for 47.4% of the hepatic sequestration for both R(+) and S(-) enantiomers. Propranolol has been shown to be stereo-selective in both its response and in its metabolism, the S(-) enantiomer being about 100 times more effective as a beta blocker than the R(+) enantiomer (Barrett and Cullum, 1968; Marier et al., 1998). Enantiomers usually vary in their biological and pharmacological effects, and beta-blockers (such as atenolol or propranolol) with a single chiral centre vary in their stereo-selectivity to bind to the β_1 or β_2 adrenergic receptors. Generally the cardiac activity is attributable to the S(-)-enantiomer which has a much higher binding affinity than its R(+)-counterpart (Barrett and Cullum, 1968; Pearson et al., 1989; Stoschitzky et al., 1993; Marier et al., 1998). It has also been suggested that the pharmacokinetics of the enantiomers *in vivo* in rabbits are comparable at lower doses but stereo-selective at higher doses, due to hepatic saturation of S(-)-propranolol clearance and that propranolol enantiomer plasma binding is not stereo-selective or dose dependent (Marier et al., 1998). In the dog, a larger distribution volume of S(-)-propranolol has

been suggested (Bai et al., 1983) and it has been shown that there is a larger uptake of S(-)-propranolol into rat heart tissue when compared to R(+)-propranolol (Kawashima et al., 1976).

The modelling of perfusate impulse-response data in our study has shown that there is a preferential uptake of the S(-)-propranolol enantiomer by the intracellular binding sites relative to R(+)-propranolol (Table 2). The kinetic parameters *PS* and K_b were found to be increased about 1.4-fold for the S(-) compared to the R(+) enantiomer, reflecting the higher binding affinity of the S(-) enantiomer for liver tissue and the rapidly equilibrating binding sites. A similar finding was evident on analysis of an *in vitro* hepatic microsomal protein binding of propranolol study (Table 3). The fraction unbound of S(-)-propranolol was found to be lower than that of R(+)-propranolol (Table 3).

Table 2 shows that the derived intrinsic elimination clearance of the S(-) enantiomer is almost 1.4-fold that compared to the R(+) isomer. This could be explained by the fact that one of the binding sites in question is microsomal protein and this binding is a prerequisite for elimination (i.e. higher microsomal binding facilitates faster elimination by microsomal metabolism). The *in vitro* metabolism data also showed that the *in vitro* CL_{int} and unbound drug fraction values for the R(+)-propranolol were significantly different (smaller CL_{int} and larger unbound drug fraction) compared to those of S(-)-propranolol (Table 3). Thus, one source of propanolol stereo-selectivity is indeed attributable to the hepatic microsomal binding differences between these two propranolol enantiomers.

Given that only 70% microsomal protein homogenised from liver tissue is metabolically active and the average production from microsomal protein of 1 g liver tissue amounts to about 50 mg

JPET Fast Forward. Published on June 10, 2004 as DOI: 10.1124/jpet.104.070011
This article has not been copyedited and formatted. The final version may differ from this version.

(Roberts and Rowland, 1986), the calculated CL_{int} values obtained from the *in vitro* microsomal protein metabolism study (Table 3) can be converted to total liver tissue CL_{int} values for R(+)-propranolol, S(-)-propranolol and RS-propranolol (7.85±0.71, 10.0±1.42, and 9.25±1.45 $ml.min^{-1}.g^{-1}$liver, respectively). These *in vitro* results are comparable to the derived CL_{int} values in an *in situ* isolated perfused liver study (R(+)-propranolol: 8.54±1.79, S(-)-propranolol: 12.1±1.56 and RS-propranolol: 11.8±2.44 $ml.min^{-1}.g^{-1}$liver, Table 2). The use of our earlier model, which does not explicitly recognise the ion-trapping of drugs by acidic organelles (Weiss et al., 2000), with the propranolol optical isomers data resulted in a fit with similar model selection criteria (compared to the present model), but with significantly larger CL_{int} values (R(+)-propranolol: 34.3±2.17, S(-)-propranolol: 43.7±5.01 and RS-propranolol: 42.2±4.87 $ml.min^{-1}.g^{-1}$liver, $p<0.001$, Fig. 4) relative to those predicted from *in vitro* microsomal data. It is therefore apparent that the contribution of ion-trapping in subcellular compartments to intracellular drug distribution must be taken into account in order to obtain a CL_{int} value that is consistent with *in vitro* metabolic values.

In addition, the vesicular ion-trapping constant K_v significantly decreased following monensin treatment for R(+)-propranolol, S(-)-propranolol and racemic propranolol (K_v control/K_v treatment: 33-, 34- and 35-fold, respectively). K_v is defined by the relative rates of permeation into and out of the acidic lysosomal and mitochondria organelles. Ion-trapping greatly reduces the permeation out of the organelles leading to an apparent large distribution space and a large K_v. Monensin abolishes the ion-trapping leading to small K_v values. The K_v value thus becomes a sensitive ion-trapping marker. Table 4 shows that the observed K_v values are very similar to theoretical values based on the likely ion-trapping of the enantiomers and racemate by acidic organelles. No differences in K_v values (i.e. extent of ion-trapping) was found between R(+) and S(-) propranolol, consistent with both enantiomers having the same pK_a value.

The relative contribution of ion-trapping, microsomal and non-specific binding and distribution of unbound drug to overall sequestration of propranolol in the liver can be estimated from a formula described in detail previously (Siebert et al., 2004). Ion-trapping, microsomal binding and unbound drug distribution account, respectively, for 47.4%, 47.1% and 5.5% of the sequestration of propranolol in the liver. Thus, ion-trapping equals intracellular binding as a key determinant of propranolol hepatic sequestration.

Sensitivity analyses (Table 5) suggest that propranolol extraction is mainly defined by metabolism, permeability and blood flow, each contributing to a similar extent. In contrast, its mean transit time is mainly defined by ion-trapping, intracellular binding, *PS* and blood flow (Table 5). No significant differences between control and monensin-treated groups were observed for hepatic extraction ratio for the propranolol optical isomers (Table 1). This finding is consistent with hepatic drug extraction being related to lipophilicity (Hung et al., 2001).

A major limitation in the present analysis is the need to restrict our modelling to sufficiently low concentrations of propranolol, to avoid saturation of metabolism or binding processes. This restriction was imposed by the inability of the physiologically based pharmacokinetic model used in this work to be applied to non-linear data. Clinically, propranolol is normally given in doses, which saturate both metabolism (von Bahr et al., 1982) and protein binding (Ludden, 1991). In addition, the binding of propranolol in the liver is also saturable (Anderson et al., 1978; Miyauchi et al., 1993). Modelling of the non-linearity of the hepatic elimination of propranolol is further complicated by the multiple metabolic pathways for propranolol and that some of the cytochrome P450 isozymes have a low affinity for propranolol whereas others have

a high affinity (Ishida et al., 1992). Work is now in progress to examine whether the parameters generated in this study can be used with non-linear propranolol data following the modelling of saturable metabolism and binding effects.

In conclusion, our study has shown that, firstly, ion-trapping contributes significantly to the hepatic disposition of propranolol. This contribution is most clearly demonstrated by the app. 34-fold decrease of K_v for R(+) and S(-) enantiomers and racemic propranolol following monensin treatment. Thus, K_v is a highly sensitive indicator of ion-trapping. Secondly, the physiologically more active S(-)-isomer showed higher hepatic CL_{int}, PS and K_b values than those of the R(+)-isomer. Thirdly, there is no difference in ion-trapping between R(+) and S(-) propranolol, consistent with these two enantiomers having the same pK_a value. Finally, monensin treatment did not affect CL_{int}, PS, K_b, or drug fraction unbound values in *in situ* liver perfusions or in *in vitro* microsomal metabolism studies for all optical isomers, implying that abolishing ion-trapping does not affect the hepatic metabolism, permeability and microsomal protein binding of propranolol.

Acknowledgements

We acknowledge the support of the National Health and Medical Research Council of Australia and the Queensland and New South Wales Lions Kidney and Medical Research Foundation. We are also grateful to Drs. Paul Mills and Melanie Thompson for their assistance in generating the data for propranolol disposition in hypoxia livers.

References

Anderson JH, Anderson RC and Iben LS (1978) Hepatic uptake of propranolol. *J Pharmacol Exp Ther* **206**:172-180.

Bai SA, Wilson MJ, Walle UK and Walle T (1983) Stereoselective increase in propranolol bioavailability during chronic dosing in the dog. *J Pharmacol Exp Ther* **227**:360-364.

Barrett AM and Cullum VA (1968) Lack of inter-action between propranolol and mebanazine. *J Pharm Pharmacol* **20**:911-915.

Cheung K, Hickman PE, Potter JM, Walker NI, Jericho M, Haslam R and Roberts MS (1996) An optimized model for rat liver perfusion studies. *J Surg Res* **66**:81-89.

Elliott SL, Morgan DJ, Angus PW, Ghabrial H and Smallwood RA (1993) The effect of hypoxia and acidosis on propranolol clearance in the isolated perfused rat liver preparation. *Biochem Pharmacol* **45**:763-765.

Hung DY, Chang P, Cheung K, McWhinney B, Masci PP, Weiss M and Roberts MS (2002) Cationic drug pharmacokinetics in diseased livers determined by fibrosis index, hepatic protein content, microsomal activity, and nature of drug. *J Pharmacol Exp Ther* **301**:1079-1087.

Hung DY, Chang P, Weiss M and Roberts MS (2001) Structure-hepatic disposition relationships for cationic drugs in isolated perfused rat livers: transmembrane exchange and cytoplasmic binding process. *J Pharmacol Exp Ther* **297**:780-789.

Ishida R, Suzuki K, Masubuchi Y, Narimatsu S, Fujita S and Suzuki T (1992) Enzymatic basis for the non-linearity of hepatic elimination of propranolol in the isolated perfused rat liver. *Biochem Pharmacol* **44**:2281-2288.

Kawashima K, Levy A and Spector S (1976) Stereospecific radioimmunoassay for propranolol isomers. *J Pharmacol Exp Ther* **196**:517-523.

Keiding S and Steiness E (1984) Flow dependence of propranolol elimination in perfused rat liver. *J Pharmacol Exp Ther* **230**:474-477.

Lalka D, Griffith RK and Cronenberger CL (1993) The hepatic first-pass metabolism of problematic drugs. *J Clin Pharmacol* **33**:657-669.

Le Couteur DG, Rivory LP and Pond SM (1993) Hepatic intracellular pH during the prereplicative period following partial hepatectomy. *Am J Physiol* **264**:G767-773.

Ludden TM (1991) Nonlinear pharmacokinetics: clinical Implications. *Clin Pharmacokinet* **20**:429-446.

Marier JF, Pichette V and du Souich P (1998) Stereoselective disposition of propranolol in rabbits. Role of presystemic organs and dose. *Drug Metab Dispos* **26**:164-169.

Miyauchi S, Sawada Y, Iga T, Hanano M and Sugiyama Y (1993) Dose-dependent hepatic handling of l-propranolol determined by multiple indicator dilution method: influence of tissue binding of l-propranolol on its hepatic elimination. *Biol Pharm Bull* **16**:1019-1024.

Pearson AA, Gaffney TE, Walle T and Privitera PJ (1989) A stereoselective central hypotensive action of atenolol. *J Pharmacol Exp Ther* **250**:759-763.

Roberts MS, Donaldson JD and Rowland M (1988) Models of hepatic elimination: comparison of stochastic models to describe residence time distributions and to predict the influence of drug distribution, enzyme heterogeneity, and systemic recycling on hepatic elimination. *J Pharmacokinet Biopharm* **16**:41-83.

Roberts MS and Rowland M (1986) Correlation between in-vitro microsomal enzyme activity and whole organ hepatic elimination kinetics: analysis with a dispersion model. *J Pharm Pharmacol* **38**:177-181.

Shand DG (1976) Pharmacokinetics of propranolol: a review. *Postgrad Med J* **52 Suppl 4**:22-25.

Siebert GA, Hung DY, Chang P and Roberts MS (2004) Ion-trapping, microsomal binding, and unbound drug distribution in the hepatic retention of basic drugs. *J Pharmacol Exp Ther* **308**:228-235.

Smallwood RH, Mihaly GW, Smallwood RA and Morgan DJ (1988) Propranolol elimination as described by the venous equilibrium model using flow perturbations in the isolated perfused rat liver. *J Pharm Sci* **77**:330-333.

Stoschitzky K, Egginger G, Zernig G, Klein W and Lindner W (1993) Stereoselective features of (R)- and (S)-atenolol: clinical pharmacological, pharmacokinetic, and radioligand binding studies. *Chirality* **5**:15-19.

Suzuki T, Ohkuma T and Isozaki S (1981) Nonlinear first-pass metabolism of propranolol in the rat. *J Pharmacobiodyn* **4**:131-141.

von Bahr C, Hermansson J and Lind M (1982) Oxidation of (R)- and (S)-propranolol in human and dog liver microsomes. Species differences in stereoselectivity. *J Pharmacol Exp Ther* **222**:458-462.

Weiss M, Kuhlmann O, Hung DY and Roberts MS (2000) Cytoplasmic binding and disposition kinetics of diclofenac in the isolated perfused rat liver. *Br J Pharmacol* **130**:1331-1338.

Weiss M and Roberts MS (1996) Tissue distribution kinetics as determinant of transit time dispersion of drugs in organs: application of a stochastic model to the rat hindlimb. *J Pharmacokinet Biopharm* **24**:173-196.

Weiss M, Stedtler C and Roberts MS (1997) On the validity of the dispersion model of hepatic drug elimination when intravascular transit time densities are long-tailed. *Bull Math Biol* **59**:911-929.

JPET Fast Forward. Published on June 10, 2004 as DOI: 10.1124/jpet.104.070011
This article has not been copyedited and formatted. The final version may differ from this version.

Figure legends

Fig. 1. Schematic overview of hepatocellular drug transport and ion-trapping (including the acidic compartment). D: drug; DH^+: protonated drug; f_{uB} is the fraction of drug unbound in perfusate; k_{in}, k_{out}, and k_e representing the permeation, efflux, and elimination rate constant, respectively; K_b is the equilibrium amount ratio characterising the rapidly equilibrating intracellular binding sites (microsomal and non-specific binding sites); k_{cv} and k_{vc} representing the rate constant for transport from cytosol into acidic vesicles (lysosomes and mitochondria) or from acidic vesicles into cytosol, respectively, determining the equilibrium amount ratio $K_v = k_{cv}/k_{vc}$ characterising the slowly accessible pool for ion-trapping; V_B is the extracellular volume (vascular + Disse space); V_C is the cellular water volume.

Fig. 2. Typical outflow profiles for the enantiomers of propranolol and [U-^{14}C]sucrose in the regressions. (**A**) R(+)-propranolol with sucrose; (**B**) S(-)-propranolol with sucrose. The solid circles represent enantiomer experiment data. The open circles represent sucrose experimental data. The lines represent the fits of the profiles.

Fig. 3. Comparison of outflow perfusion concentration-time profiles and regression lines obtained from the two-phase physiologically based organ pharmacokinetic model for (**A**) racemic propranolol, (**B**) R(+)-propranolol and (**C**) S(-)-propranolol in controls and following monensin treatment. Solid circles represent controls and open circles represent treatment. Solid and dashed lines stand for fitted data in control and treatments, respectively.

Fig. 4. Comparison of intrinsic elimination clearance (CL_{int}) values obtained from the *in vitro* microsomal protein metabolism study, derived from the modified two-phase physiologically based organ pharmacokinetic model (with an additional ion-trapping parameter, K_v) and derived from the earlier two-phase organ model (without K_v) for the enantiomers of propranolol and racemic propranolol fitting in an *in situ* isolated perfused liver study.

Table 1 Non-parametric moments for the enantiomers of propranolol and racemic propranolol (mean ± SD, n = 6).

Drug	Hepatic extraction ratio (E)		Mean transit time (MTT, sec)		Normalized variance (CV^2)	
	Control[a]	Treatment[b]	Control	Treatment	Control	Treatment
R(+)-Propranolol	0.96 ± 0.05	0.93 ± 0.07	109 ± 24.3	78.3 ± 15.7	1.16 ± 0.27	0.87 ± 0.31
S(-)-Propranolol	0.97 ± 0.02	0.90 ± 0.09	121 ± 18.5	75.1 ± 18.4	1.23 ± 0.39	0.78 ± 0.43
RS-Propranolol	0.96 ± 0.03	0.93 ± 0.06	119 ± 20.3	79.5 ± 15.3	1.07 ± 0.25	0.86 ± 0.39

[a]before monensin treatment. [b]after monensin treatment. Two-way analysis of variance showed there was no significant difference between the control and treatment groups for the three isomers for E and CV^2 values and significant differences for the MTT value between the control and treatment groups. Further, Tukey post-hoc test showed there was no significant difference between the three isomers for the MTT value both in the control and treatment groups.

Table 2 Kinetic parameters derived from the physiologically based two-phase organ pharmacokinetic model fitting for the enantiomers of propranolol and racemic propranolol (mean ± SD, n = 6).

Drug	[a]K_v		[b]CL_{int} (mL min^{-1} g^{-1}liver)		[c]PS (mL min^{-1} g^{-1}liver)		[d]K_b	
	Control	Treatment	Control	Treatment	Control	Treatment	Control	Treatment
R(+)-Propranolol	8.20 ± 0.64	0.25	8.54 ± 1.79	8.17 ± 1.33	25.4 ± 3.42	29.5 ± 7.39	7.39 ± 0.64	7.39 ± 0.64
S(-)-Propranolol	8.54 ± 1.06	0.25	12.1 ± 1.56	11.01 ± 2.03	37.2 ± 8.72	37.9 ± 8.49	8.87 ± 1.20	8.87 ± 1.20
RS-Propranolol	8.79 ± 1.79	0.25	11.8 ± 2.44	12.1 ± 2.31	35.9 ± 8.64	37.2 ± 9.07	8.65 ± 1.13	8.65 ± 1.13

[a]K_v: equilibrium amount ratio characterising the vesicular ion-trapping sites. [b]CL_{int}: intrinsic elimination clearance. [c]PS: permeability-surface area product. [d]K_b: equilibrium amount ratio characterising the intracellular binding sites. Two-way analysis of variance showed there was no significant difference between the control and treatment groups for the three isomers for CL_{int}, PS and K_b values and significant differences for the K_v value between the control and treatment groups. Further, Tukey post-hoc test showed CL_{int}, PS and K_b values for R(+)-propranolol were significant differences to those of S(-)-propranolol ($p<0.05$) and RS-propranolol ($p<0.05$) but no difference for the K_v value for the three isomers both in the control and treatment groups; no significant difference was found to exist between S(-)-propranolol and RS-propranolol for all kinetic parameters.

JPET Fast Forward. Published on June 10, 2004 as DOI: 10.1124/jpet.104.070011
This article has not been copyedited and formatted. The final version may differ from this version.

Table 3 *In vitro* microsomal protein (MP) binding and metabolism of the enantiomers of propranolol and racemic propranolol (mean ± SD, n = 4).

Drug	[a]$f_{u,MP}$		[b]CL_{int} (mL min^{-1} mg^{-1}MP)	
	Control	Treatment	Control	Treatment
R(+)-Propranolol	0.57 ± 0.01	0.59 ± 0.05	0.11 ± 0.01	0.10 ± 0.02
S(-)-Propranolol	0.51 ± 0.04	0.50 ± 0.03	0.14 ± 0.02	0.14 ± 0.02
RS-Propranolol	0.49 ± 0.05	0.47 ± 0.04	0.13 ± 0.02	0.13 ± 0.01

[a]$f_{u,MP}$: drug fraction unbound. [b]CL_{int}: intrinsic elimination clearance. Two-way analysis of variance showed there was no significant difference between the control and treatment groups for the three isomers for $f_{u,MP}$ and CL_{int} values. Further, Tukey post-hoc test showed significant differences between $f_{u,MP}$ and CL_{int} values of R(+)-propranolol compared to those of S(-)-propranolol ($p<0.05$) and RS-propranolol ($p<0.05$) but no significant difference was found to exist between S(-)-propranolol and RS-propranolol for the control and treatment groups.

Table 4. Comparison of predicted and observed model derived K_v (equilibrium amount ratio characterising the vesicular ion-trapping sites) for propranolol optical isomers.

Drug	pK_a	[a]Lysosomes to intracellular concentration ratio (l:i)	[a]Mitochondria to intracellular concentration ratio (m:i)	[b]Predicted K_v	[c]Observed model derived K_v
R(+)-Propranolol	9.45	736	3.96	8.16	8.20±0.64
S(-)-Propranolol	9.45	736	3.96	8.16	8.54±1.06
RS-Propranolol	9.45	736	3.96	8.16	8.79±1.79

[a]vesicle to cytosol concentration ratio = $\frac{1+10^{pKa-pHv}}{1+10^{pKa-pHi}}$ (Goldstein *et al.*, 1974), where pHi ≈ 7.27 is the cytosolic pH (Le Couteur *et al.*, 1993), pHv ≈ 4.4 is the lysosomes pH (Daniel, 2003), pHv ≈ 6.67 is the mitochondria pH in the fasted state (Soboll *et al.*, 1980). [b]Given that the fraction of lysosomes (f_{lyso}) and mitochondria (f_{mito}) to cytosol is 1% and 20% (Rhoades and Pflanzer, 1996), the overall unbound drug vesicles/intracellular distribution ratio (v:i) for propranolol can be estimated from the individual organelle volume fraction and concentration ratio above using the equation: $K_v = f_{lyso}$ x l:i + f_{mito} x m:i. [c]data fitting results using the physiologically based two-phase organ pharmacokinetic model.

JPET Fast Forward. Published on June 10, 2004 as DOI: 10.1124/jpet.104.070011
This article has not been copyedited and formatted. The final version may differ from this version.

Table 5 Sensitivity analysis of effects of changes in model parameters describing the disposition of propranolol in rat liver controls on hepatic extraction ratio (*E*) and mean transit time (*MTT*) for RS- propranolol (mean ± SD, n = 6). Model independent moment derived estimates from Table 1 are shown in italics for comparison.

Effects of change in model parameter	*E*	*MTT* (sec)
[a]*Observed control (with acidic vesicles) data*	*0.96 ± 0.03*	*119 ± 20.3*
[b]Simulated control data	0.92 ± 0.03	124 ± 20.8
[a]*Observed treated (no acidic vesicles) data*	*0.93 ± 0.06*	*79.5 ± 15.3*
[b]Simulated treated data ([c]K_v = 0.25)	0.92 ± 0.03	[i]73.8 ± 23.5
[b]Simulated with [d]K_b reduced by 50%	0.92 ± 0.03	[h]80.9 ± 17.6
[b]Simulated with [e]k_e reduced by 50%	[h]0.81 ± 0.06	115 ± 20.1
[b]Simulated with [f]Q reduced by 50%	[h]0.78 ± 0.06	95.8 ± 24.3
[b]Simulated with [g]PS reduced by 50%	[h]0.74 ± 0.08	91.7 ± 27.7

[a]data obtained from non-parametric moments analysis (Table 1). [b]simulation using Equation (4) or (5). [c]K_v: ion-trapping parameter. [d]K_b: intracellular binding:. [e]k_e: metabolism. [f]Q: blood flow. [g]PS: permeability-surface area product. [h, i]:Tukey post-hoc differences between observed data and various simulations ([h]: $p<0.05$; [i]: $p<0.01$).

Figure 1

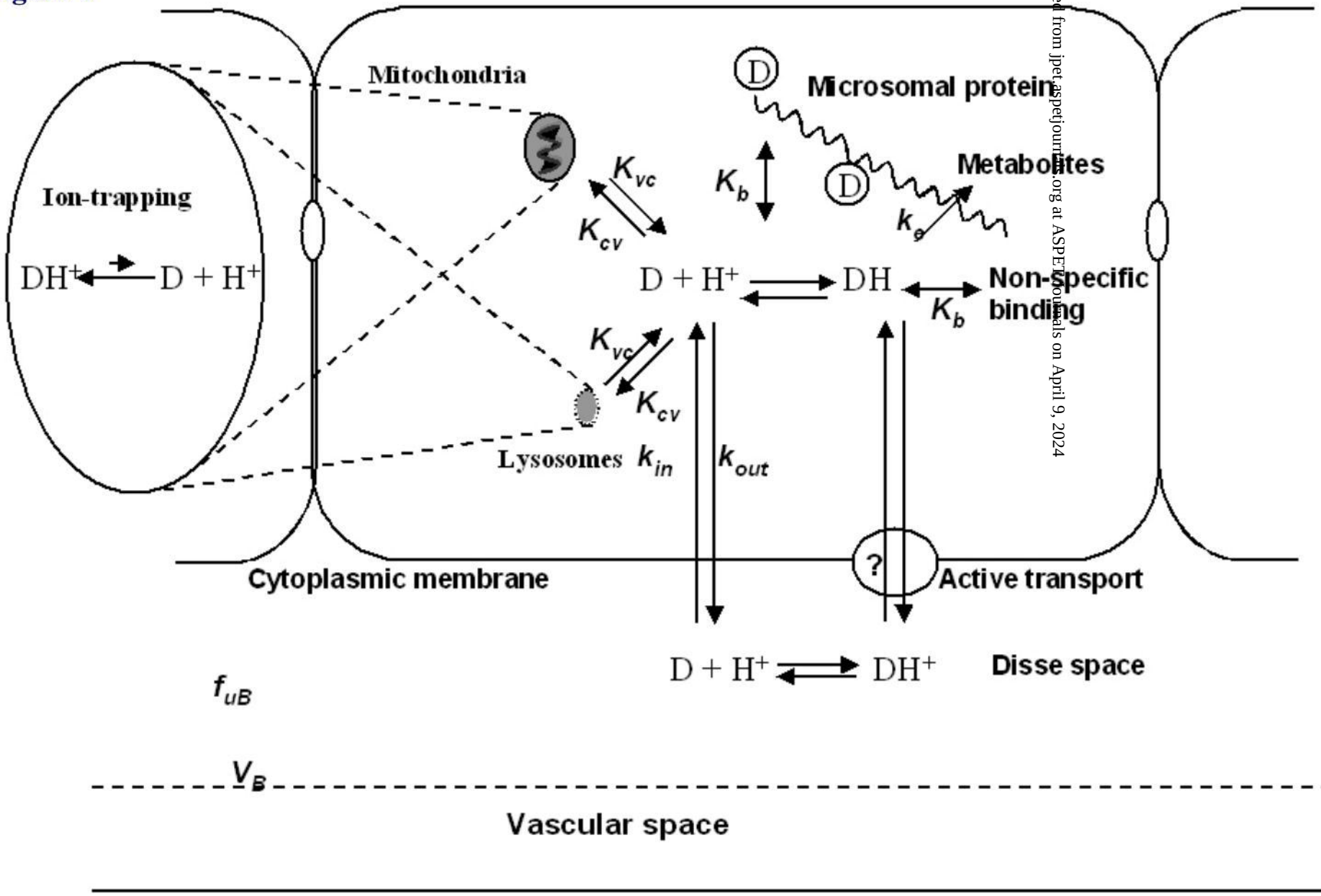

Figure 2A

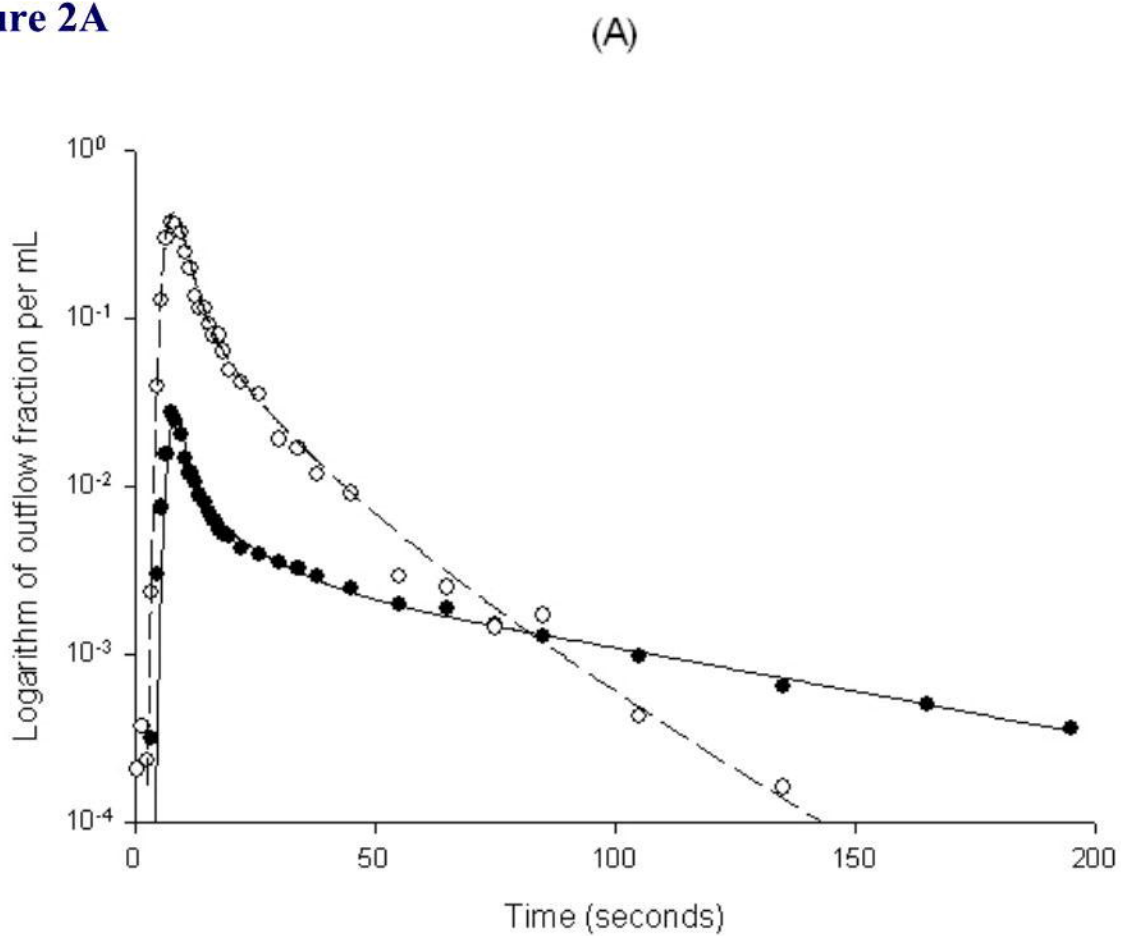
(A)
Logarithm of outflow fraction per mL
10⁰
10⁻¹
10⁻²
10⁻³
10⁻⁴
0
50
100
150
200
Time (seconds)

Figure 2B

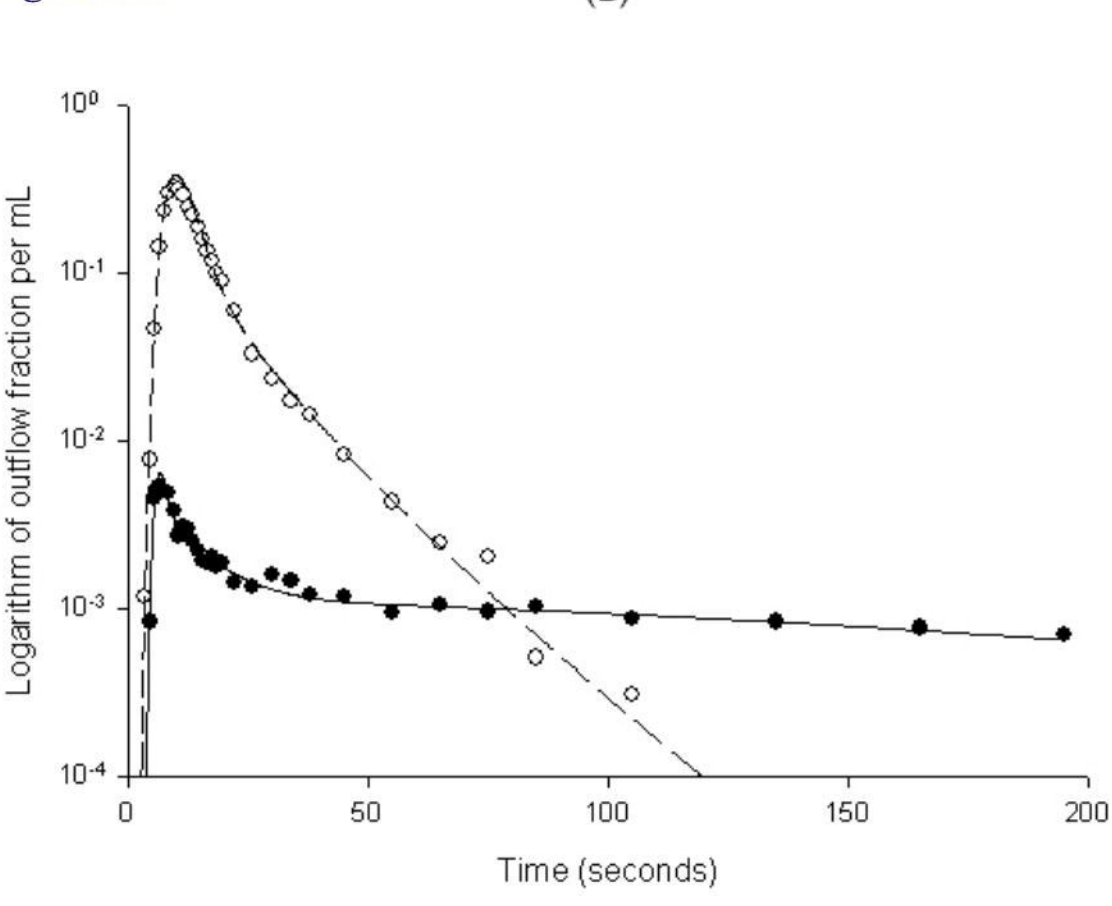
(B)
Logarithm of outflow fraction per mL
10⁰
10⁻¹
10⁻²
10⁻³
10⁻⁴
0
50
100
150
200
Time (seconds)

Figure 3A

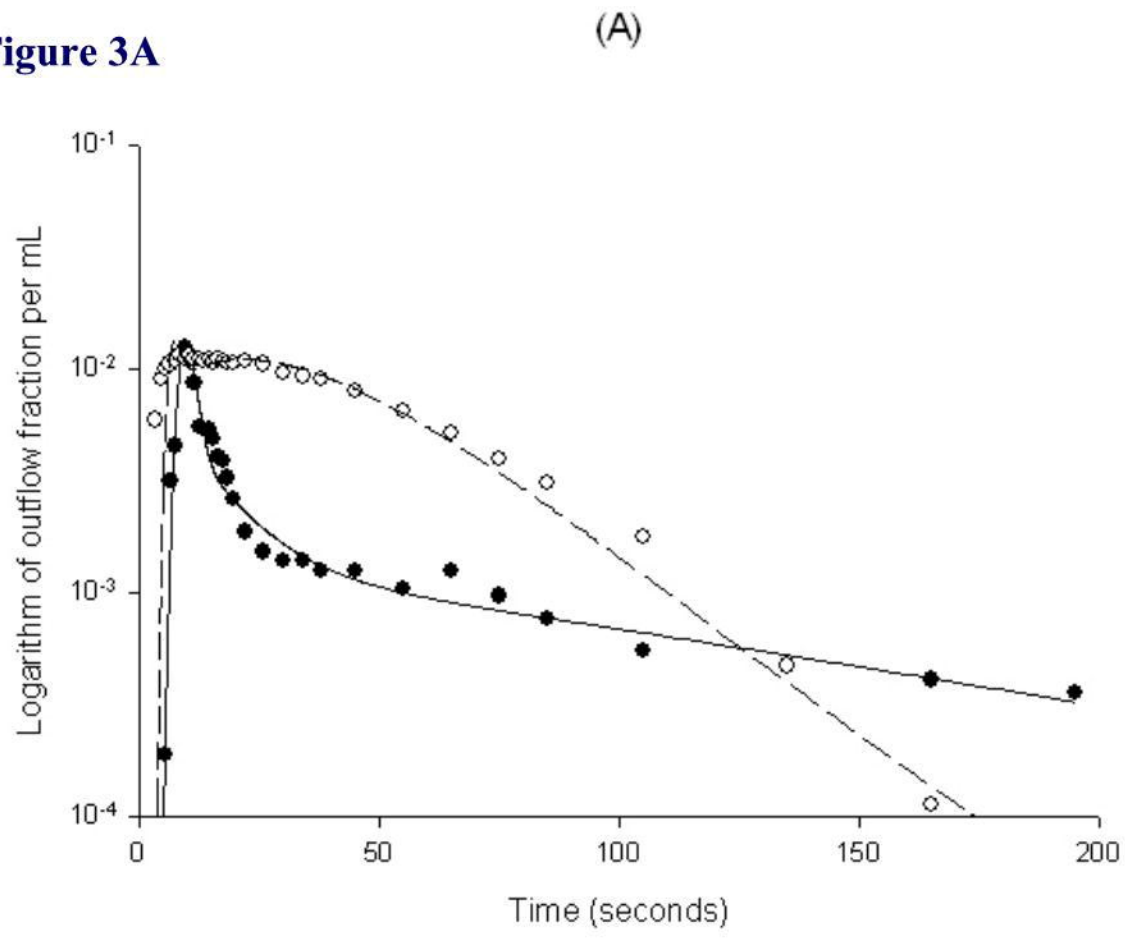
(A)
Logarithm of outflow fraction per mL
10-1
10-2
10-3
10-4
0
50
100
150
200
Time (seconds)

Figure 3B

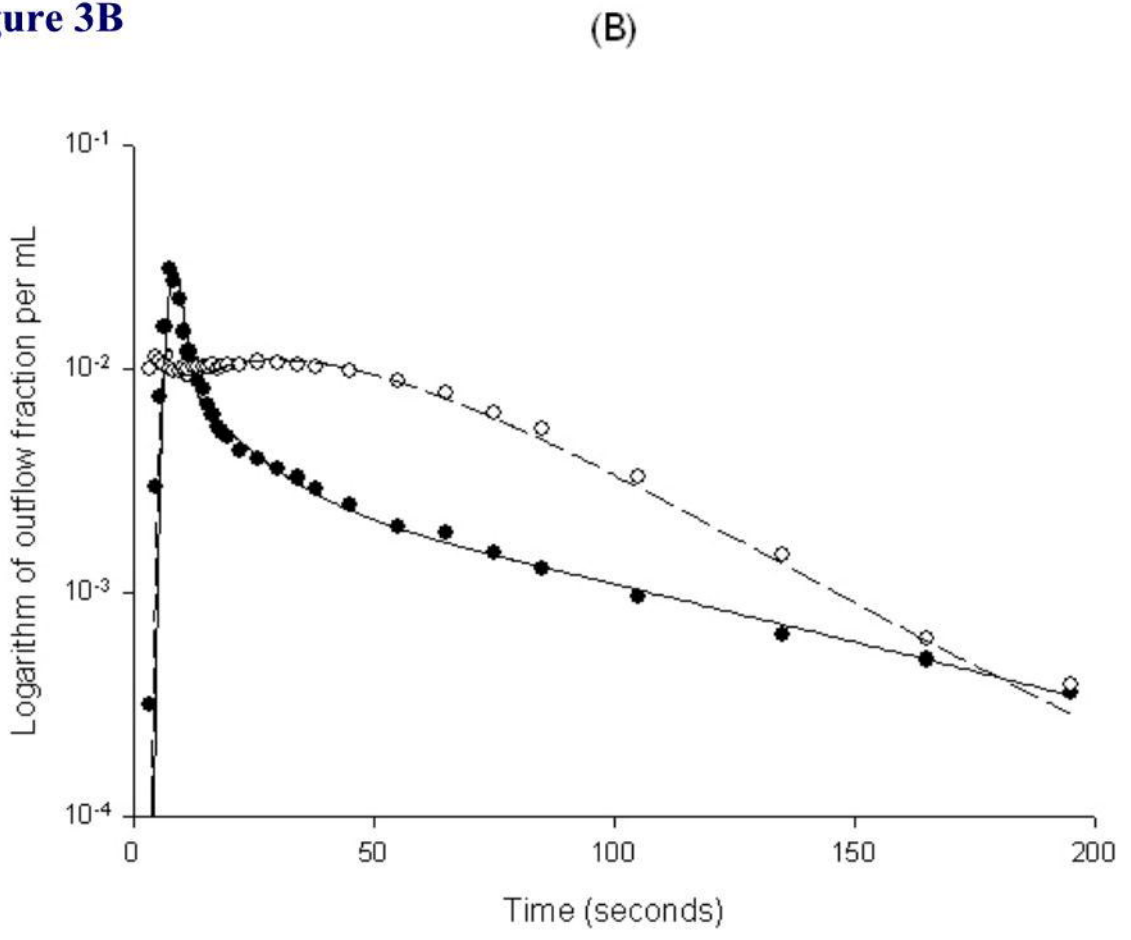
(B)
Logarithm of outflow fraction per mL
10-1
10-2
10-3
10-4
0
50
100
150
200
Time (seconds)

Figure 3C

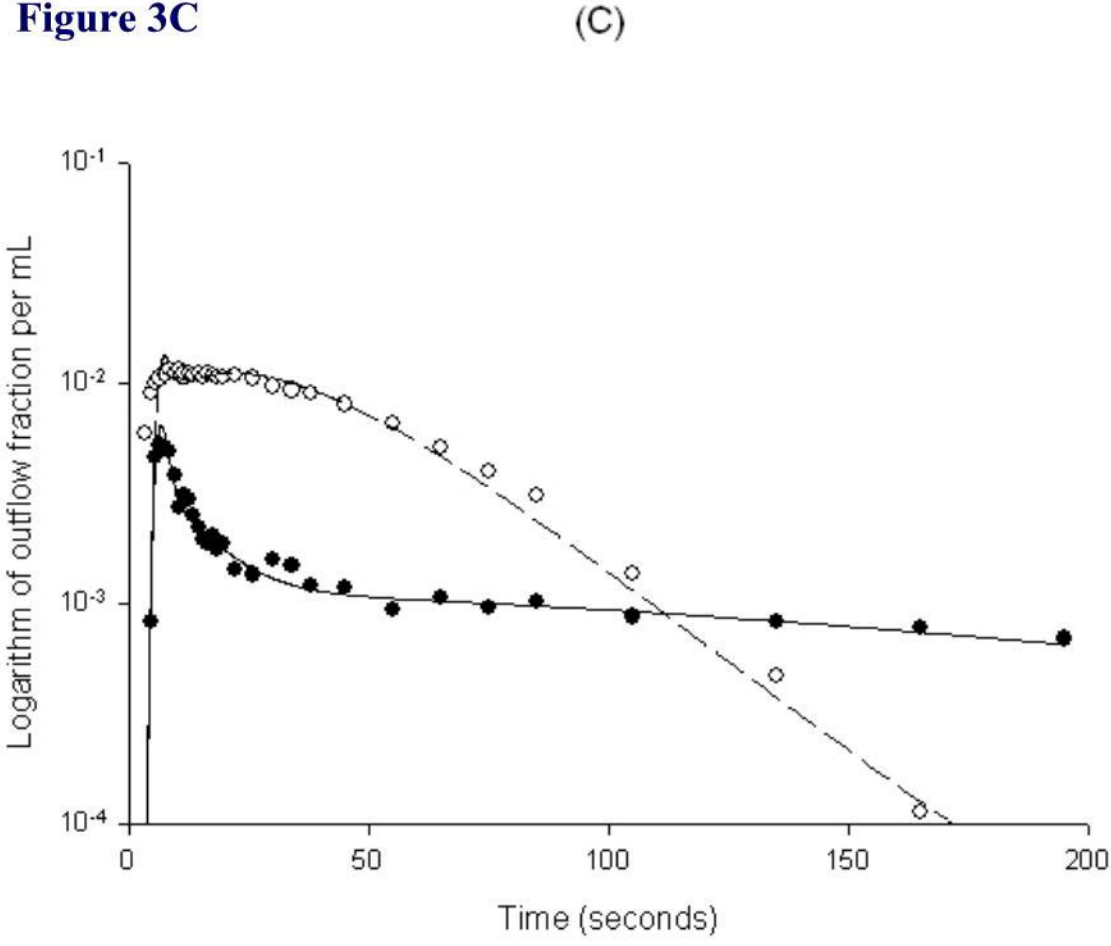
(C)
Logarithm of outflow fraction per mL
10-1
10-2
10-3
10-4
0
50
100
150
200
Time (seconds)

Figure 4

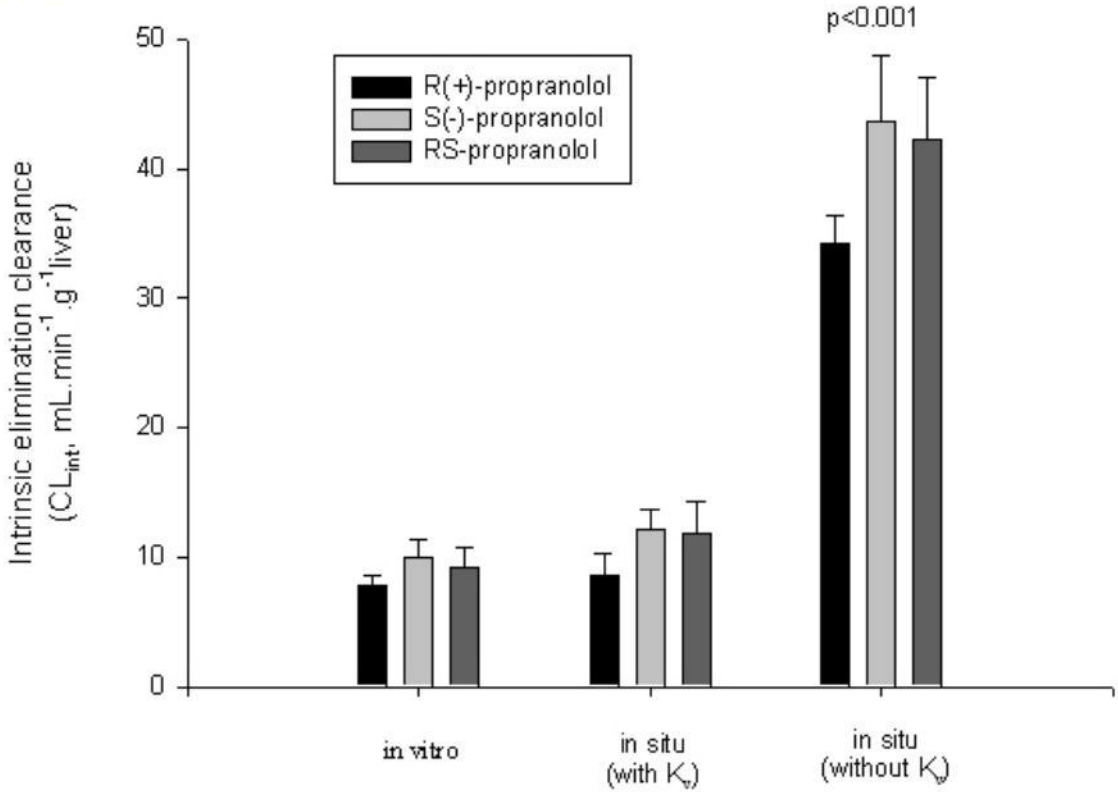
p<0.001
R(+)-propranolol
S(-)-propranolol
RS-propranolol
Intrinsic elimination clearance
(CL_{int}, $mL.min^{-1}.g^{-1}$ liver)
50
40
30
20
10
0
in vitro
in situ
(with K_p)
in situ
(without K_p)